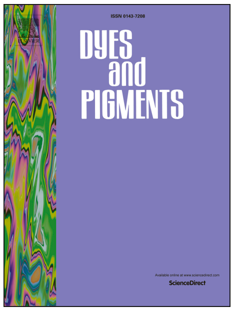

Aggregation-induced emission (AIE)-active highly emissive novel carbazole-based dyes with various solid-state fluorescence and reversible mechanofluorochromism characteristics

Fei Zhao, Zhao Chen, Congbin Fan, Gang Liu, Shouzhi Pu

PII: S0143-7208(18)32576-2
DOI: https://doi.org/10.1016/j.dyepig.2019.01.057
Reference: DYPI 7330

To appear in: *Dyes and Pigments*

Received Date: 22 November 2018
Revised Date: 17 January 2019
Accepted Date: 18 January 2019

Please cite this article as: Zhao F, Chen Z, Fan C, Liu G, Pu S, Aggregation-induced emission (AIE)-active highly emissive novel carbazole-based dyes with various solid-state fluorescence and reversible mechanofluorochromism characteristics, *Dyes and Pigments* (2019), doi: https://doi.org/10.1016/j.dyepig.2019.01.057.

Aggregation-induced emission (AIE)-active highly emissive novel carbazole-based dyes with various solid-state fluorescence and reversible mechanofluorochromism characteristics

Fei Zhao, Zhao Chen**, Congbin Fan, Gang Liu, Shouzhi Pu*

Synopsis

Three carbazole-based fluorescent molecules were successfully synthesized. These luminogens showed color-tunable solid-state fluorescence, high thermal stability, typical aggregation-induced emission, and reversible mechanofluorochromism characteristics.

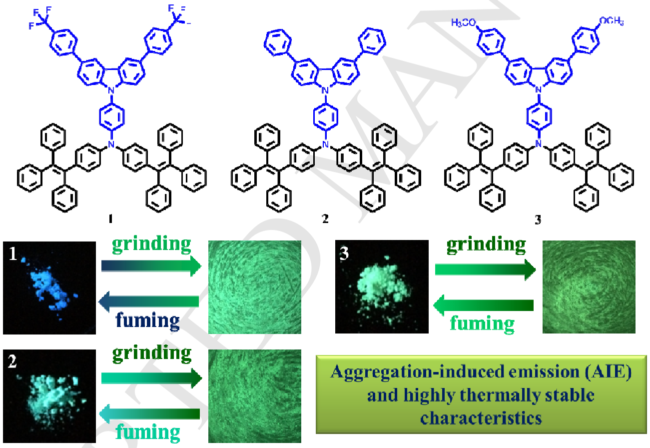

Aggregation-induced emission (AIE)-active highly emissive novel carbazole-based dyes with various solid-state fluorescence and reversible mechanofluorochromism characteristics

Fei Zhao, Zhao Chen**, Congbin Fan, Gang Liu, Shouzhi Pu*

Jiangxi Key Laboratory of Organic Chemistry, Jiangxi Science and Technology Normal University, Nanchang 330013, PR China.

Tel: +86-791-83831996   Fax: +86-791-83831996

** Corresponding author E-mail: chenzhao666@126.com

* Corresponding author E-mail: pushouzhi@tsinghua.org.cn

ABSTRACT

Three new carbazole-based fluorescent molecules **1**-**3** functionalized with tetraphenylethene have been successfully synthesized, and these compounds have high thermal stability, and they exhibited different fluorescence in solid states with the superior luminescence quantum yields of 99.04% (**1**), 98.90% (**2**) and 39.83% (**3**). Their aggregation-induced behaviors were explored by the study of photoluminescence spectroscopy. The results showed that luminogens **1**-**3** exhibited remarkable aggregation-induced emission effect. Furthermore, their distinct mechanical stimulus-responsive fluorescence characteristics were also surveyed by solid-state photoluminescence spectroscopy. Interestingly, the various emitting colors of these luminogens could be changed into the same green, and the repeatabilities of their mechanochromic luminescence behaviors were outstanding, and the powder X-ray diffraction results indicated that the reversible conversion from a crystalline to an amorphous state was responsible for the obvious mechanofluorochromism phenomena of compounds **1**-**3**. This work will be valuable for the exploitation of mechanical-force sensors with typical aggregation-induced emission feature.

Keywords: Carbazole; Tetraphenylethene; High thermal stability; Different fluorescence; Aggregation-induced emission; Mechanofluorochromism

1. Introduction

Organic luminescence materials exhibiting bright fluorescence in the solid state have received considerable attention in recent decades in view of their promising applications in optoelectronic devices, sensors and display devices [1-6]. In particular, mechanofluorochromic functionalized materials, displaying different luminescent colors induced by mechanical force, have been attracting continuing interests from researchers because of their broad applications in the fields of pressure sensors, data storage and rewritable media [7-17]. Generally, the molecular packing of mechanochromic luminescence molecules can be adjusted by various intermolecular interactions such as π-π interactions, hydrogen bonding and halogen bonding, and no chemical structure damage appear in mechanofluorochromic luminogens during their reversible luminescence change processes [18-24]. To date, numerous mechanical stimulus-responsive materials have been reported. However, the types of the corresponding mechanochromic materials are limited, and examples of high-efficiency mechanochromic smart fluorescent materials with obvious color change before and after stimulating are still inadequate. Indeed, a lot of effort has been made to exploit high-contrast mechanofluorochromic materials. There is no doubt that strong solid-state emission is a crucial factor for the development of mechanochromism materials with clear color contrast. Unfortunately, the majority of traditional emissive materials exhibit very bright luminescence in their dilute solutions, but the bright luminescence is often weakened or quenched at high concentrations, a well-known phenomenon referred to as aggregation-caused quenching (ACQ) [25], and the ACQ effect largely hinders the exploitation of high-performance mechanical force-responsive materials. Excitingly, Tang *et al.* discovered the aggregation-induced emission (AIE) phenomenon [26], which is commonly caused by the restriction of intramolecular motions[27,28]. Luminophors with AIE effect can overcome ACQ, and achieve strong solid-state emission. Indeed, the exploitation of AIE-active fluorogenic molecules has attracted intense research interest due to their potential applications in the fields of biomedical imaging, sensors and organic light emitting diode [29-37]. For example, AIE-active fluorogens can be designed to exhibit very weak fluorescence in aqueous media, and their fluorescence will be turned on upon interacting with target analytes, which is extremely significative for biosensing and imaging applications of these fluorogenic molecules with AIE feature. Until now, luminogens simultaneously possessing AIE and reversible mechanochromism characteristics are still scarce, not to mention highly thermal stable luminogens with these interesting properties. Therefore, the discovery of AIE-active mechanochromic highly thermal stable compounds is a significative and challenging research topic, and it deserves great attention.

Carbazole-based derivatives are very valuable candidates in the fields of photoelectronic devices and sensors [38-45]. Nevertheless, the notorious ACQ effect limits the rapid development of these materials with carbazole skeletons. Thus, it is also a very important and urgent challenge to synthesize AIE-active luminogens based on a carbazole scaffold structure. In this work, we designed and prepared three novel carbazole-based tetraphenylethene derivatives with different substituents (Chart 1). Aggregation-induced behavior and mechanofluorochromic feature of these highly emissive dyes were systematically investigated by photoluminescence spectroscopy, dynamic light scattering and powder X-ray diffraction. Indeed, all these different solid-state light-emitting compounds showed superior thermal stability, outstanding AIE and reversible mechanochromic fluorescence characteristics.

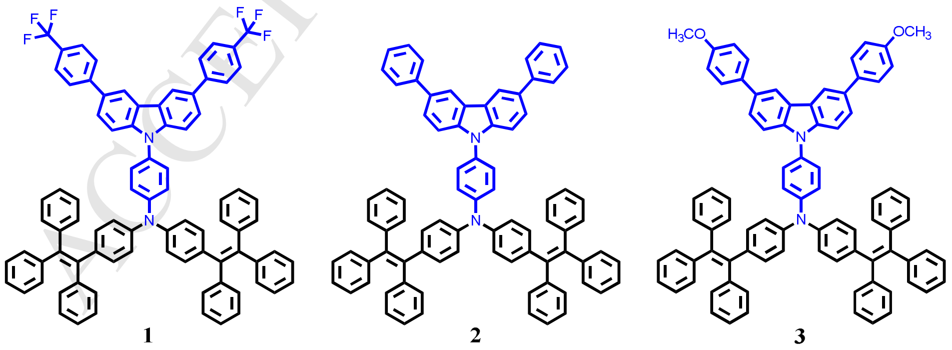

Chart 1. The molecular structures of carbazole-based compounds **1-3**.

2. Materials and methods

2.1. Experimental

General: All manipulations were carried out under an argon atmosphere by using standard Schlenk techniques, unless otherwise stated. The starting materials 3,6-dibromo-9H-carbazole, (4-(trifluoromethyl)phenyl)boronic acid, phenylboronic acid, (4-methoxyphenyl)boronic acid, n-(4-iodophenyl)acetamide, nitrobenzene and tetrabutylammonium bromide (TBAB) purchased from J&K Chemical were used as received. All other starting materials and reagents were obtained as analytical-grade from commercial suppliers and used without further purification. Compounds **1-1** [46], **1-2** [46], **1-3** [46] and **1-4** [47] were prepared by procedures described in the corresponding literatures. ^{1}H NMR (400 MHz) and ^{13}C NMR (100 MHz) spectra were collected on American Varian Mercury Plus 400 spectrometer (400 MHz). ^{1}H NMR spectra were reported as followed: chemical shift in ppm (δ) relative to the chemical shift of TMS at 0.00 ppm, integration, multiplicities (s = singlet, d = doublet, t = triplet, m = multiplet), and coupling constant (Hz). ^{13}C NMR chemical shifts reported in ppm (δ) relative to the central line of triplet for $CDCl_3$ at 77 ppm, Mass spectra were obtained on a Bruker AmaZon SL Ion Trap Mass spectrometer. Elemental analyses (C, H, N) were carried out with a PE CHN 2400 analyzer. The absorption spectra were measured on an Agilent 8453 UV/Vis spectrophotometer. Fluorescence spectra were recorded on a Hitachi-F-4600 fluorescence spectrophotometer. XRD studies were recorded on a Shimadzu XRD-6000 diffractometer using Ni-filtered and graphite-monochromated Cu Kα radiation (λ = 1.54 Å, 40 kV, 30 mA). The N, N-dimethyl formamide (DMF)/water mixtures with various water fractions were prepared by slowly adding ultra-pure water into the

DMF solution of samples. Absolute fluorescence quantum yields and fluorescence lifetimes were measured by Edinburgh FLS1000 spectrometer. Dynamic light scattering (DLS) measurements were performed by NanoBrook 90Plus (Brookhaven Instruments). Column chromatographic separations were carried out on silica gel (200-300 mesh). TLC was performed by using commercially prepared 100-400 mesh silica gel plates (GF254) and visualization was effected at 254 nm.

2.2. Synthesis

*2.2.1. Synthesis of compounds **1**, **2** and **3**.* Into a 50 mL, two-necked, round-bottom flask were placed **1-4** (1234 mg, 3.0 mmol), $Pd_2(dba)_3$ (57.4 mg, 0.1 mmol), and *t*-BuONa (384.4 mg, 4.0 mmol). The flask was evacuated under a vacuum and then flushed with dry nitrogen three times. Toluene (30 ml), **1-1** (546.5 mg, 1.0 mmol) or **1-2** (410.5 mg, 1.0 mmol) or **1-3** (470.6 mg, 1.0 mmol), and toluene solution of $(t\text{-}Bu)_3P$ (2 ml) were injected into the flask, and the mixture was refluxed for 48 h and then cooled to room temperature. The solution was poured into water (60 ml) and extracted with dichloromethane three times. The combined organic layers were washed with brine, dried (Na_2SO_4), and concentrated in vacuo. In the end, the residues were purified by silica-gel column chromatography, affording the expected solid product **1** (white), **2** (yellowish) or **3** (yellow) in a yield of 80%, 75% or 76%, respectively. **1:** ^1H NMR (400 MHz, $CDCl_3$): δ (ppm) = 8.42 (s, 2H), 7.83 (d, *J* = 8 Hz, 4H), 7.74-7.68 (m, 6H), 7.50 (d, *J* = 8 Hz, 2H), 7.38 (d, *J* = 8 Hz, 2H), 7.20-7.03 (m, 32H), 6.96-6.88 (m, 8H). ^{13}C NMR (100.6 MHz, $CDCl_3$): δ (ppm) = 147.2, 145.4, 145.3, 144.0, 143.6, 143.5, 141.6, 140.9, 140.5, 139.0, 132.4, 132.1, 131.4, 131.3, 130.6, 129.2, 128.9, 128.6, 128.2, 127.7, 127.7, 127.6, 127.5, 126.5, 126.4, 125.8, 124.0, 123.8, 123.7, 123.1, 119.1, 110.6. ESI-MS (m/z): 1207.3 $[M]^+$. Anal. Calcd. for $C_{84}H_{56}F_6N_2$: C, 83.56; H, 4.68; N, 2.32. Found: C, 83.49; H, 4.76; N, 2.26. **2:** ^{1}H NMR (400 MHz, $CDCl_3$): δ (ppm) = 8.39 (s, 2H), 7.74-7.67 (m, 6H), 7.48 (t, *J* = 8 Hz, 6H), 7.41-7.33 (m, 4H), 7.19-7.03 (m, 32H), 6.95-6.87 (m, 8H). ^{13}C NMR (100.6 MHz, $CDCl_3$): δ (ppm) = 146.8, 145.4, 144.0, 143.7, 143.5, 142.0, 141.0, 140.8, 140.6, 138.8, 133.5, 132.3, 131.4, 128.8, 127.7, 127.6, 127.5, 127.3, 126.6, 126.5, 126.4, 126.4, 125.6, 124.1, 123.9, 123.5, 118.8, 110.2. ESI-MS (m/z): 1071.4 $[M]^+$. Anal. Calcd. for $C_{82}H_{58}N_2$: C, 91.93; H, 5.46; N, 2.61. Found: C, 91.98; H, 5.50; N, 2.54. **3:** ^{1}H NMR (400 MHz, $CDCl_3$): δ (ppm) = 8.33 (d, *J* = 4 Hz, 2H), 7.67-7.61 (m, 6H), 7.46-7.38 (m, 4H), 7.18-7.02 (m, 36H), 6.95-6.87 (m, 8H), 3.88 (s, 6H). ^{13}C NMR (100.6 MHz, $CDCl_3$): δ (ppm) = 158.7, 146.7, 145.4, 144.0, 143.7, 143.5, 140.8, 140.7, 140.6, 138.8, 134.7, 133.1, 132.3, 131.4, 128.3, 127.7, 127.6, 127.5, 126.5, 126.4, 126.4, 125.3, 124.2, 123.9, 123.5, 118.4, 114.3, 110.2, 55.4. ESI-MS (m/z): 1131.4 $[M]^+$. Anal. Calcd. for $C_{84}H_{62}N_2O_2$: C, 89.17; H, 5.52; N, 2.48. Found: C, 89.10; H, 5.61; N, 2.43.

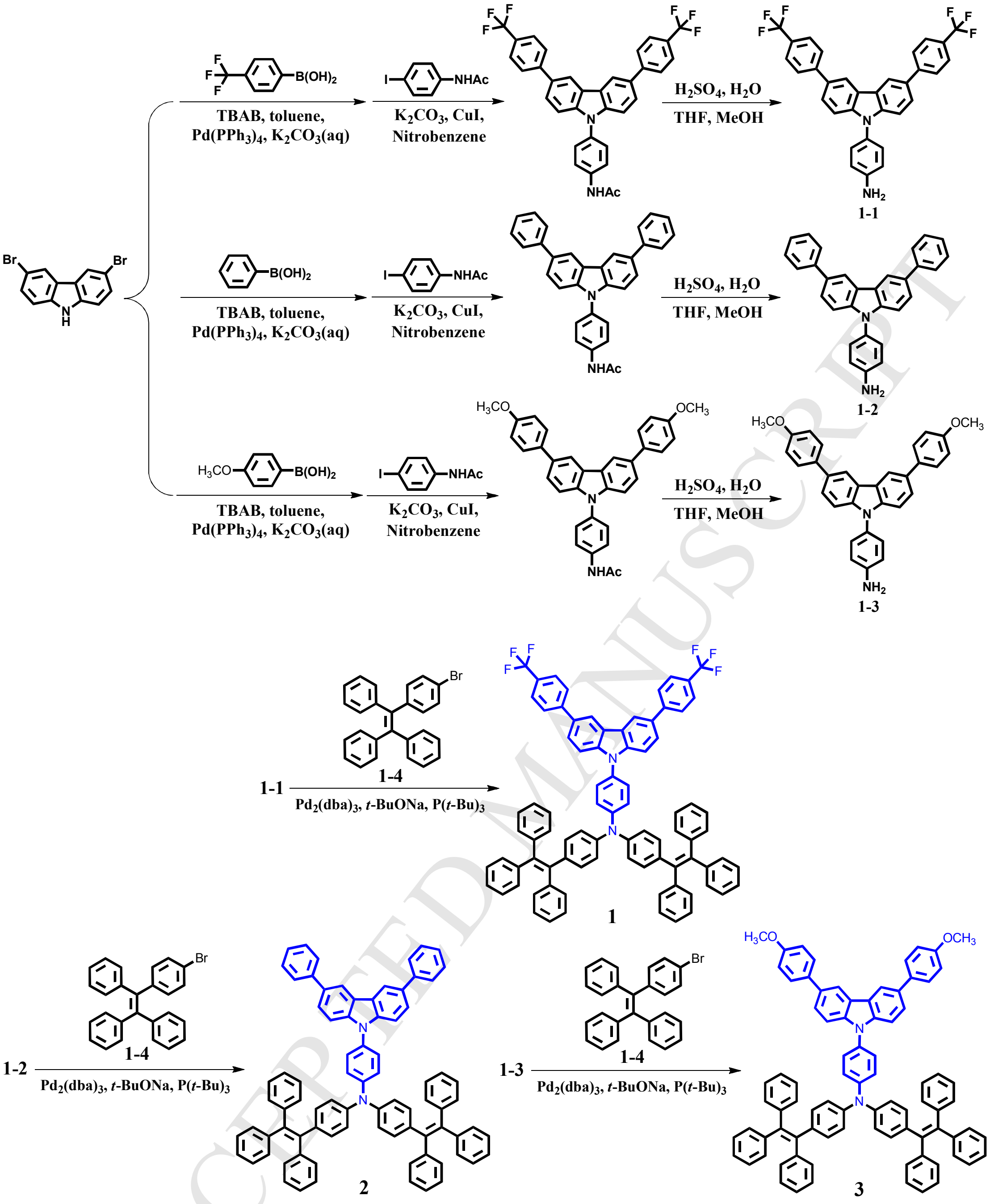

Scheme 1. Synthesis routes of compounds **1-3**.

3. Results and discussion

3.1. Synthesis

As shown in Scheme 1, the carbazole-based tetraphenylethene derivatives with different substituents were prepared in 80%, 75% or 76% yield respectively according to the substitution reaction of intermediate product **1-1**, **1-2** or **1-3** and intermediate product **1-4**.

*3.2. Aggregation-induced emission (AIE) characteristics of compounds **1-3***

To investigate the AIE behaviors of compounds **1**-**3**, the UV-Vis absorption spectra of luminogens **1**-**3** (20 μM) in DMF-H_2O mixtures with different water fractions (f_w) were studied initially (Supporting information: Figs. S1-S3). Indeed, level-off tails in the visible region were observed as the f_w increased. This interesting phenomenon is commonly associated with the well-known Mie scattering effect, and it is the signal of nano-aggregate formation [48]. Next, the photoluminescence (PL) spectra of **1**-**3** (20 μM) in DMF-H_2O mixtures with various water contents were systematically explored. As can be seen in Fig. 1, luminogens **1**-**3** are almost non-emissive in pure DMF, and the corresponding fluorescence quantum yield is 1.15% for **1**, 0.48% for **2**, or 2.03% for **3**, respectively. However, when the water content in the DMF solution was increased to 30%, a new green emission band was observed, with a maximum (λ_{max}) at 505 nm for **1**, 507 nm for **2**, or 508 nm for **3**, and a strong green luminescence with the related fluorescence quantum yield up to 68.01% (**1**), 67.92% (**2**) or 59.90% (**3**) could be observed as the f_w value was increased to 90%.

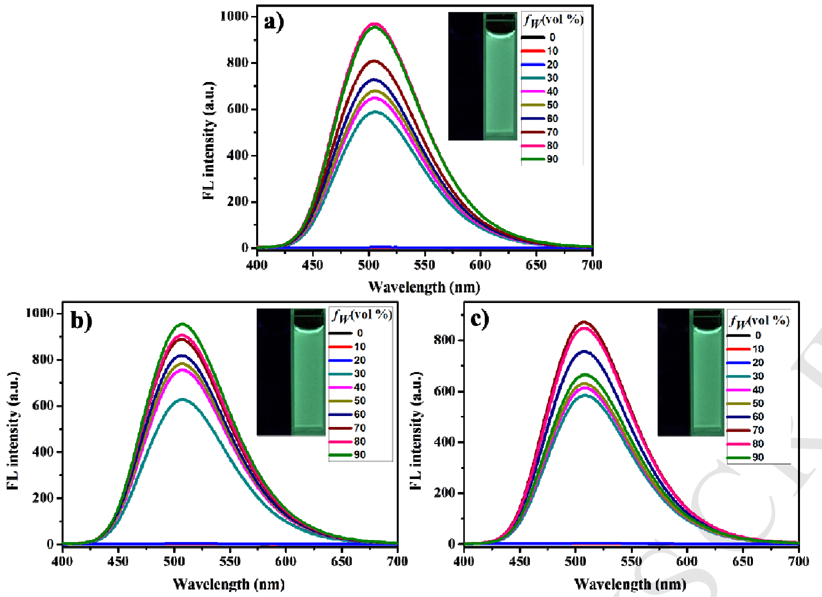

Fig. 1. PL spectra of the dilute solutions (2.0 × 10^{-5} mol L^{-1}) of luminogen **1** (a), **2** (b) or **3** (c) in DMF-H_2O mixtures with various water contents (0%-90%). Excitation wavelength = 365 nm. The inset shows the corresponding fluorescence images of **1** (a), **2** (b) or **3** (c) in pure DMF as well as 90% water fraction under 365 nm UV light.

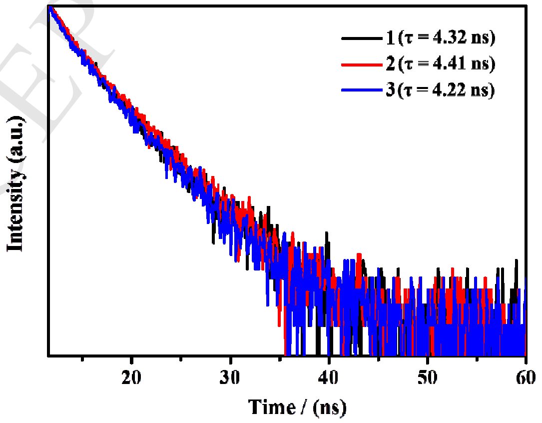

Fig. 2. Decay curves of luminogens **1-3** **(**505 nm for **1**, 507 nm for **2** and **3**) in DMF-water mixtures with 90% volume fraction of water. Concentration：2.0 × 10^{-5}

mol L^{-1}.

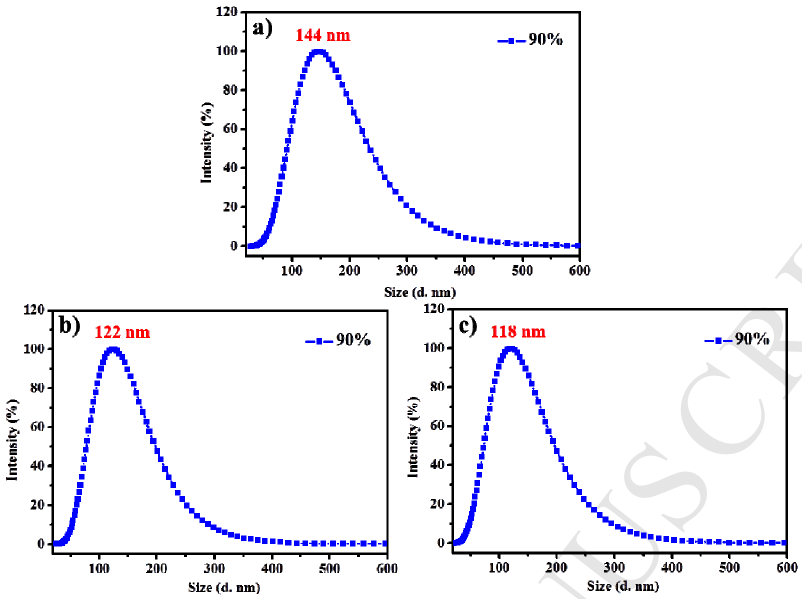

Fig. 3. Size distribution curves of **1** (a), **2** (b) and **3** (c) in DMF-water mixtures with 90% volume fraction of water. Concentration: 2.0×10^{-5} mol L^{-1}.

In addition, as shown in Fig. 2, the emission lifetime of **1**, **2** or **3** in 90% water fraction is 4.32 ns, 4.41 ns or 4.22 ns, respectively. There is no doubt that water is a nonsolvent for luminogens **1-3**, and thus an increase in the water content of mixed solvent caused the aggregate formation. In fact, the nano-aggregates obtained were characterized by dynamic light scattering (DLS) experiments (Fig. 3). Therefore, the bright green fluorescence of **1-3** was attributed to aggregate formation. Clearly, **1-3** belong to AIE-active luminous molecules.

*3.3. Solid-state fluorescence characteristics and thermal stability of compounds **1-3***

To investigate the solid-state fluorescence behaviors of luminogens **1-3**, the solid-state PL spectra of **1-3** were studied.

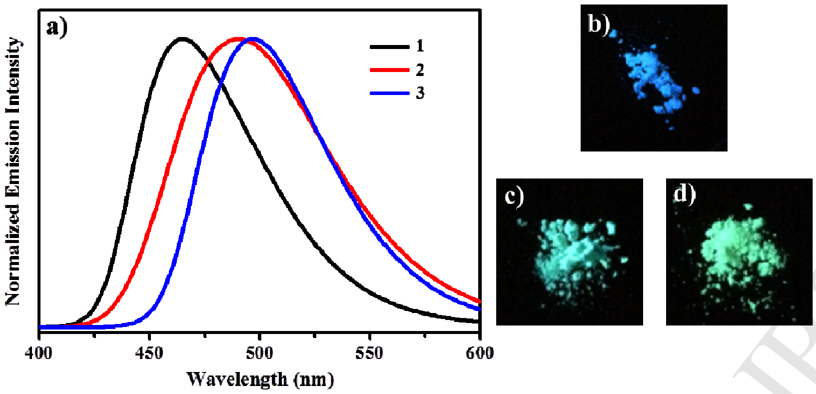

Fig. 4. (a) Solid-state PL spectra of compounds **1**-**3**. The fluorescence images of luminogens **1**-**3** under 365 nm UV light: (b) the solid sample of **1**; (c) the solid sample of **2**; (d) the solid sample of **3**.

As evident from Fig. 4, the emission spectrum of **1** with two trifluoromethyl groups showed an emission band with λ_{max} at 465 nm, corresponding to a blue emission under 365 nm UV light, and **2** showed a broad emission band with λ_{max} at 490 nm, and it exhibited blue-green fluorescence upon UV illumination at 365 nm. However, **3** with two methoxyl groups exhibited green luminescence with a λ_{max} at 497 nm. On the other hand, to evaluate the thermostability of the compounds **1**-**3**, their thermogravimetric analyses (TGA) were carried out. As presented in Fig. 5, luminogens **1**-**3** are thermally stable and possess high onset degradation temperatures (T_d) ranging from 480 to 540℃.

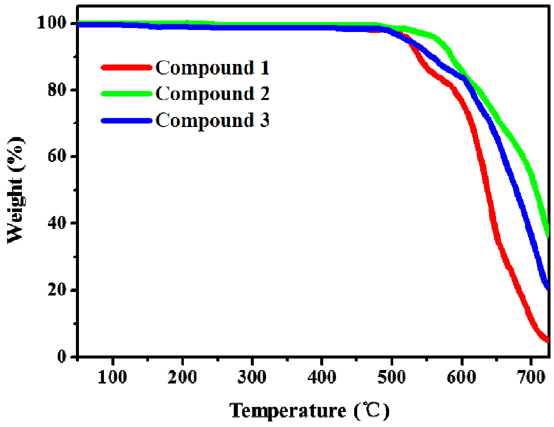

Fig. 5. TGA thermograms of solid samples **1-3**.

*3.4. The mechanofluorochromic behaviors of compounds **1-3***

Subsequently, the mechanochromic fluorescence characteristics of compounds **1-3** were further researched by PL spectroscopy. As shown in Fig. 6, the solid sample of **1** showed blue luminescence, and its fluorescence quantum yield (QY) is 99.04%. However, upon grinding of the corresponding solid sample using a pestle, a new emission peak with $\lambda_{\max}$ at 510 nm was observed, and the strong blue emission was converted into the green luminescence (QY = 61.92%). Meanwhile, as shown in Fig. S4, the emission lifetime of before or after grinding is 2.52 ns or 2.50 ns, respectively. On the other hand, upon treatment of the ground sample with dichloromethane solvent, the green-emitting sample could be reverted to its initial blue color. Therefore, **1** exhibited obvious and reversible mechanofluorochromic behavior. Furthermore, this reversible mechanochromic fluorescence could be repeated numerous times without obvious changes by repeated grinding-exposure (Fig. S5). The possible mechanism of mechanofluorochromic phenomenon of **1** was examined by powder X-ray diffraction (PXRD) experiment. As can be seen in Fig. 7, the XRD pattern of the as-synthesized sample exhibited a lot of sharp diffraction peaks, indicative of its crystalline nature. Interestingly, after grinding, the clear and sharp reflection peaks vanished, which implied that grinding resulted in the transformation from a crystalline to an amorphous state. In contrast, the original intense diffraction peaks reappeared after treatment by exposure to dichloromethane vapor, suggesting that the crystalline phase was restored. Thus, the PXRD measurements indicated that a crystal-to-amorphous phase conversion was responsible for the reversible mechanofluorochromism phenomenon of compound **1**. Consistent with the mechanochromic behavior of **1**, as shown in Fig. 8 and Fig. 9, compounds **2** and **3** also showed similar mechanochromic fluorescence characteristics, and their emission lifetimes of before and after grinding are shown in Fig. S6 and Fig. S9. Moreover, the repeatabilities of their mechanofluorochromic behaviors were also excellent (Fig. S7 and Fig. S10). In addition, as presented in Fig. S8 and Fig. S11, the mechanism of their mechanofluorochromism phenomena was also attributed to the switchable morphology changes between the crystalline and amorphous states.

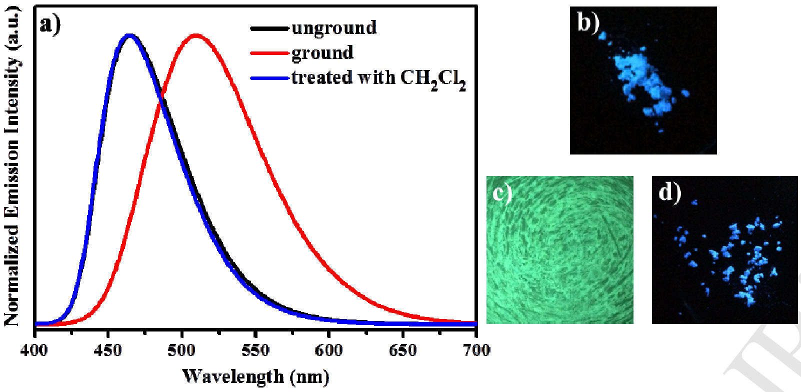

Fig. 6. (a) Solid-state PL spectra of compound **1** before grinding, after grinding, and after treatment with dichloromethane vapor. Excitation wavelength: 365 nm. Photographic images of **1** under 365 nm UV illumination: (b) the unground solid sample. (c) the ground solid sample. (d) the solid sample after treatment with dichloromethane vapor.

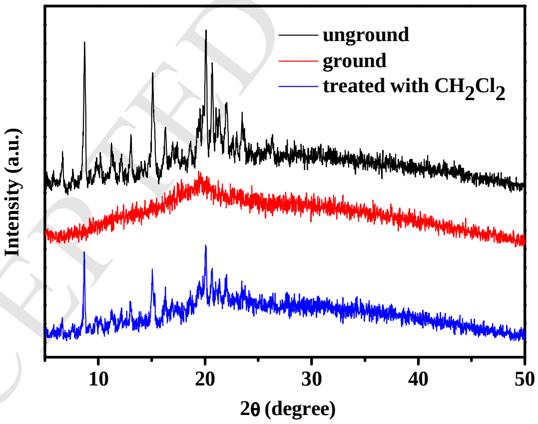

Fig. 7. XRD patterns of compound **1**: unground, ground and after treatment with dichloromethane vapor.

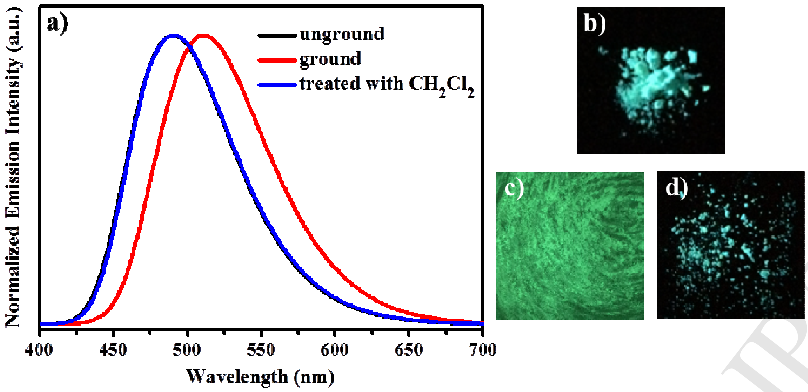

Fig. 8. (a) Solid-state PL spectra of compound **2** before grinding, after grinding, and after treatment with dichloromethane vapor. Excitation wavelength: 365 nm. Photographic images of **2** under 365 nm UV illumination: (b) the unground solid sample. (c) the ground solid sample. (d) the solid sample after treatment with dichloromethane vapor.

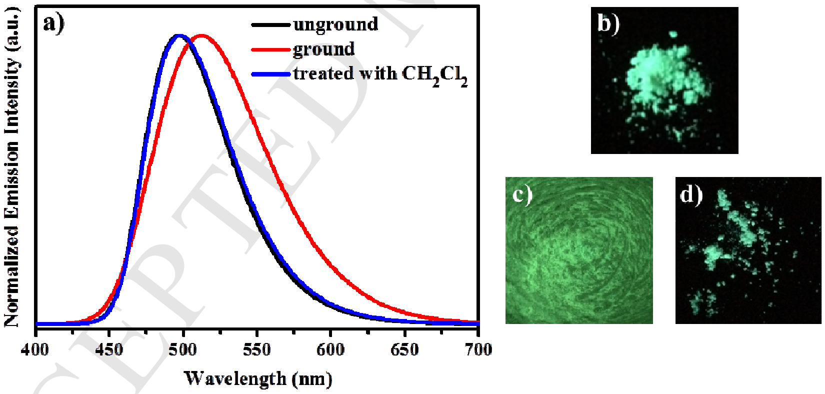

Fig. 9. (a) Solid-state PL spectra of compound **3** before grinding, after grinding, and after treatment with dichloromethane vapor. Excitation wavelength: 365 nm. Photographic images of **3** under 365 nm UV illumination: (b) the unground solid sample. (c) the ground solid sample. (d) the solid sample after treatment with dichloromethane vapor.

4. Conclusions

In summary, three novel carbazole-based tetraphenylethene-containing luminogens with different substituents were designed and synthesized to investigate their AIE, solid-state fluorescence, thermal stability, and mechanofluorochromic characteristics. Noteworthily, compounds **1**-**3** showed high thermal stability and bright solid-state fluorescence with outstanding luminescence quantum yield of 99.04%, 98.90% or 39.83%, and their solid-state emission could be adjusted by various substituents. Furthermore, luminogens **1**-**3** showed typical AIE effect. In addition, **1**-**3** also exhibited reversible mechanofluorochromism phenomena. Indeed, the various solid-state emitting colors of these luminogens could be changed into the same green, and the repeatabilities of their mechanochromic fluorescence behaviors were excellent. The PXRD results indicated that the reversible conversion from a crystalline to an amorphous state was responsible for the reversible mechanofluorochromic characteristics of **1**-**3**. This work will be beneficial for the exploitation of highly thermally stable mechanical-force sensors with AIE feature.

Acknowledgments

The authors are grateful for the financial support from the National Natural Science Foundation of China (21702079), the “5511” Science and Technology Innovation Talent Project of Jiangxi Province (20165BCB18015), the key project of Natural Science Foundation of Jiangxi Province (20171ACB20025), the youth project of Natural Science Foundation of Jiangxi Province (20171BAB213004), the

Young Talents Project of Jiangxi Science and Technology Normal University (2017QNBJRC005), and the Project of the Science Fund of Jiangxi Education Office (GJJ180593).

Supporting Information Available

UV/visible-absorbance spectra of compounds **1-3** (2.0×10^{-5} mol L^{-1}) in DMF-water mixtures with various water contents (0-90%). Solid-state PL spectra and photographic images of compounds **2** and **3** in various solid states. Decay curves of compounds **2** and **3** in various solid states. Repetitive experiments of mechanochromic behaviors for compounds **2** and **3**. XRD patterns of compounds **2** and **3** in various solid states, and Copies of NMR spectra and Mass spectra.

References

[1] Woodward AN, Kolesar JM, Hall SR, Saleh NA, Jones DS, Walter MG. Thiazolothiazole fluorophores exhibiting strong fluorescence and viologen-like reversible electrochromism. J Am Chem Soc 2017;139:8467-73.

[2] Chen Z, Wu D, Han X, Liang J, Yin J, Yu GA, et al. A novel fluorene-based gold(I) complex with aggregate fluorescence change: a single-component white light-emitting luminophor. Chem Commun 2014;50:11033-5.

[3] Xie Z, Chen C, Xu S, Li J, Zhang Y, Liu S, et al. White-light emission strategy of a single organic compound with aggregation-induced emission and delayed fluorescence properties. Angew Chem Int Ed 2015;54:7181-4.

[4] Chow PK, Cheng G, Tong GSM, Ma C, Kwok WM, Ang WH, et al. Highly luminescent palladium(II) complexes with sub-millisecond blue to green

phosphorescent excited states. Photocatalysis and highly efficient PSF-OLEDs. Chem Sci 2016;7:6083-98.

[5] Chen Z, Liang J, Han X, Yin J, Yu GA, Liu SH. Fluorene-based novel highly emissive fluorescent molecules with aggregate fluorescence change or aggregation-induced emission enhancement characteristics. Dyes Pigm 2015;112:59-66.

[6] Gao N, Cheng C, Yu C, Hao E, Wang S, Wang J, et al. Facile synthesis of highly fluorescent BF_2 complexes bearing isoindolin-1-one ligand. Dalton Trans 2014; 43:7121-7.

[7] Chen Z, Zhang J, Song M, Yin J, Yu GA, Liu SH. A novel fluorene-based aggregation-induced emission (AIE)-active gold(I) complex with crystallization-induced emission enhancement (CIEE) and reversible mechanochromism characteristics. Chem Commun 2015;51:326-9.

[8] Chi Z, Zhang X, Xu B, Zhou X, Ma C, Zhang Y, et al. Recent advances in organic mechanofluorochromic materials. Chem Soc Rev 2012;41:3878-96.

[9] Chen Z, Liu G, Pu S, Liu SH. Bipyridine-based aggregation-induced phosphorescent emission (AIPE)-active gold(I) complex with reversible phosphorescent mechanochromism and self-assembly characteristics. Dyes Pigm 2018;152:54-9.

[10] Chen W, Wang S, Yang G, Chen S, Ye K, Hu Z, et al. Dicyanomethylenated acridone based crystals: torsional vibration confinement induced emission with supramolecular structure dependent and stimuli responsive characteristics. J Phys

Chem C 2016;120:587-97.

[11] Tzeng BC, Chang TY, Wei SL, Sheu HS. Reversible phase transformation and mechanochromic luminescence of Zn^{II}-dipyridylamide-based coordination frameworks. Chem Eur J 2012;18:5105-12.

[12] Dong YQ, Lam JWY, Tang BZ. Mechanochromic luminescence of aggregation-induced emission luminogens. J Phys Chem Lett 2015;6:3429-36.

[13] Santhiya K, Sen SK, Natarajan R, Shankar R, Murugesapandian B. D-A-D structured bis-acylhydrazone exhibiting aggregation-induced emission, mechanochromic luminescence, and Al(III) detection. J Org Chem 2018;83:10770-5.

[14] Wang Y, Xu D, Gao H, Wang Y, Liu X, Han A, et al. Twisted donor-acceptor cruciform luminophores possessing substituent-dependent properties of aggregation-induced emission and mechanofluorochromism. J Phys Chem C 2018;122:2297-306.

[15] Wang Y, Xu D, Gao H, Wang Y, Liu X, Han A, et al. Mechanofluorochromic properties of aggregation-induced emission-active tetraphenylethene-containing cruciform luminophores. Dyes Pigm 2018;156:291-8.

[16] Gao H, Xu D, Wang Y, Zhang C, Yang Y, Liu X, et al. Aggregation-induced emission and mechanofluorochromism of tetraphenylbutadiene modified β-ketoiminate boron complexes. Dyes Pigm 2018;150:165-73.

[17] Xu D, Hao J, Gao H, Wang Y, Wang Y, Liu X, et al. Twisted donor-acceptor cruciform fluorophores exhibiting strong solid emission, efficient aggregation-induced emission and high contrast mechanofluorochromism. Dyes Pigm 2018;150:293-300.

[18] Chen Z, Liang J, Nie Y, Xu X, Yu GA, Yin J, et al. A novel carbazole-based gold(I) complex with interesting solid-state, multistimuli-responsive characteristics. Dalton Trans 2015;44:17473-7.

[19] Dong Y, Xu B, Zhang J, Tan X, Wang L, Chen J, et al. Piezochromic luminescence based on the molecular aggregation of 9,10-bis((*E*)-2-(pyrid-2-yl)vinyl)anthracene. Angew Chem Int Ed 2012;51:10782-5.

[20] Tan R, Wang S, Lan H, Xiao S. Polymorphism-dependent and mechanochromic luminescent molecules. Curr Org Chem 2017;21:236-48.

[21] Ito H, Saito T, Oshima N, Kitamura N, Ishizaka S, Hinatsu Y, et al. Reversible mechanochromic luminescence of $[(C_6F_5Au)_2(\mu\text{-}1,4\text{-diisocyanobenzene})]$. J Am Chem Soc 2008;130:10044-5.

[22] Mehlana G, Wilkinson C, Ramon G, Bourne SA. Reversible thermo- and mechanochromic behaviour in a 3D hydrogen bonded discrete complex. Polyhedron 2015;98:224-9.

[23] Ni J, Zhang X, Qiu N, Wu YH, Zhang LY, Zhang J, et al. Mechanochromic luminescence switch of platinum(II) complexes with 5-trimethylsilylethynyl-2,2'-bipyridine. Inorg Chem 2011;50:9090-6.

[24] Zhao KY, Shan GG, Fu Q, Su ZM. Tuning emission of AIE-active organometallic Ir(III) complexes by simple modulation of strength of donor/acceptor on ancillary ligands. Organometallics 2016;35:3996-4001.

[25] Hong Y, Lam JWY, Tang BZ. Aggregation-induced emission. Chem Soc Rev 2011;40:5361-88.

[26] Luo J, Xie Z, Lam JWY, Cheng L, Chen H, Qiu C, et al. Aggregation-induced emission of 1-methyl-1,2,3,4,5-pentaphenylsilole. Chem Commun 2001;1740-1.

[27] Mei J, Hong Y, Lam JWY, Qin A, Tang Y, Tang BZ. Aggregation-induced emission: the whole is more brilliant than the parts. Adv Mater 2014;26:5429-79.

[28] Mei J, Leung NLC, Kwok RTK, Lam JWY, Tang BZ. Aggregation-induced emission: together we shine, united we soar! Chem Rev 2015;115:11718-940.

[29] Liu J, Lam JWY, Tang BZ. Acetylenic polymers: syntheses, structures, and functions. Chem Rev 2009;109:5799-867.

[30] Long Z, Liu M, Jiang R, Wan Q, Mao L, Wan Y, et al. Preparation of water soluble and biocompatible AIE-active fluorescent organic nanoparticles via multicomponent reaction and their biological imaging capability. Chem Eng J 2017;308:527-34.

[31] Zhang X, Wang K, Liu M, Zhang X, Tao L, Chen Y, et al. Polymeric AIE-based nanoprobes for biomedical applications: recent advances and perspectives. Nanoscale 2015;7:11486-508.

[32] Li J, Kwon N, Jeong Y, Lee S, Kim G, Yoon J. Aggregation-induced fluorescence probe for monitoring membrane potential changes in mitochondria. ACS Appl Mater Interfaces 2018;10:12150-4.

[33] Zhang X, Zhang X, Yang B, Liu M, Liu W, Chen Y, et al. Polymerizable aggregation-induced emission dye-based fluorescent nanoparticles for cell imaging applications. Polym Chem 2014;5:356-60.

[34] Zhang X, Zhang X, Yang B, Liu M, Liu W, Chen Y, et al. Fabrication of

aggregation induced emission dye-based fluorescent organic nanoparticles via emulsion polymerization and their cell imaging applications. Polym Chem 2014;5:399-404.

[35] Huang H, Liu M, Wan Q, Jiang R, Xu D, Huang Q, et al. Facile fabrication of luminescent hyaluronic acid with aggregation-induced emission through formation of dynamic bonds and their theranostic applications. Mater Sci Eng C 2018;91:201-7.

[36] Jiang R, Liu M, Chen T, Huang H, Huang Q, Tian J, et al. Facile construction and biological imaging of cross-linked fluorescent organic nanoparticles with aggregation-induced emission feature through a catalyst-free azide-alkyne click reaction. Dyes Pigm 2018;148:52-60.

[37] Mao L, Liu Y, Yang S, Li Y, Zhang X, Wei Y. Recent advances and progress of fluorescent bio-/chemosensors based on aggregation-induced emission molecules. Dyes Pigm 2019;162:611-23.

[38] Huang M, Li Y, Wu K, Luo J, Xie G, Li L, et al. Carbazole-dendronized thermally activated delayed fluorescent molecules with small singlet-triplet gaps for solution-processed organic light-emitting diodes. Dyes Pigm 2018;153:92-8.

[39] Xu J, Yang Y, Hu L, Guo T, Zhang B, Yang W, et al. Blue light-emitting polymers containing *ortho*-linking carbazole-based benzothiophene-*S*, *S*-dioxide derivative. Dyes Pigm 2017;138:245-54.

[40] Chen Z, Li Z, Hu F, Yu GA, Yin J, Liu SH. Novel carbazole-based aggregation-induced emission-active gold(I) complexes with various mechanofluorochromic behaviors. Dyes Pigm 2016;125:169-78.

[41] Dong S, Li Z, Qin J. New carbazole-based fluorophores: synthesis, characterization, and aggregation-induced emission enhancement. J Phys Chem B 2009;113:434-41.

[42] Wen P, Gao Z, Zhang R, Li A, Zhang F, Li J, et al. A-π-D-π-A carbazole derivatives with remarkable solvatochromism and mechanoresponsive luminescence turn-on. J Mater Chem C 2017;5:6136-43.

[43] Chen Z, Liu G, Pu S, Liu SH. Carbazole-based aggregation-induced emission (AIE)-active gold(I) complex: Persistent room-temperature phosphorescence, reversible mechanochromism and vapochromism characteristics. Dyes Pigm 2017;143:409-15.

[44] Cai S, Shi H, Zhang Z, Wang X, Ma H, Gan N, et al. Hydrogen-bonded organic aromatic frameworks for ultralong phosphorescence by intralayer π-π interactions. Angew Chem Int Ed 2018;57:4005-9.

[45] Chen Z, Liu G, Pu S, Liu SH. Triphenylamine, carbazole or tetraphenylethylene-based gold(I) complexes: Tunable solid-state room-temperature phosphorescence and various mechanochromic luminescence characteristics. Dyes Pigm 2018;159:499-505.

[46] Kimoto A, Cho JS, Higuchi M, Yamamoto K. Synthesis of asymmetrically arranged dendrimers with a carbazole dendron and a phenylazomethine dendron. Macromolecules 2004;37:5531-7.

[47] Zhao F, Fan C, Chen Z, Liu G, Pu S. Cyanobenzene-containing tetraphenylethene derivatives with aggregation-induced emission and self-recovering

mechanofluorochromic characteristics. RSC Adv 2017;7:43845-8.

[48] Leung CWT, Hong Y, Chen S, Zhao E, Lam JWY, Tang BZ. A photostable AIE luminogen for specific mitochondrial imaging and tracking. J Am Chem Soc 2013;135:62-5.

Highlights

- Three novel carbazole-based tetraphenylethene-containing compounds were synthesized.
- All these compounds showed high thermal stability and strong solid-state fluorescence.
- These luminogens exhibited typical aggregation-induced emission characteristics.
- These luminogens with different substituents exhibited color-tunable solid-state fluorescence.
- These luminogens exhibited highly reversible mechanofluorochromic behaviors.